



ELSEVIER

January 2000

**MATERIALS
LETTERS**

Materials Letters 42 (2000) 113–120

www.elsevier.com/locate/matlet

Nanocrystalline bismuth synthesized via an in situ polymerization–microemulsion process

Jiye Fang, Kevin L. Stokes^{*}, Joan Wiemann, Weilie Zhou*Advanced Materials Research Institute, University of New Orleans, New Orleans, LA 70148, USA*

Received 22 June 1999; accepted 1 July 1999

Abstract

Nanometer-sized bismuth particles were prepared using an inverse microemulsion method. To prevent air-oxidation, an in situ polymerization technique using methyl methacrylate (monomer) and 2-hydroxyethyl methacrylate (co-monomer) with cross-link agent was employed, and polymeric network was formed around the water droplets. Our characterizations reveal that very highly crystalline bismuth particles on the order of 20 nm can be obtained within this polymeric network. Comparison with a similar microemulsion procedure without polymer indicates that the polymeric network protected the bismuth particles against oxidation, especially during post-synthesis annealing. The current investigation demonstrates a feasible route to produce single phase, air-sensitive metal nanocrystallites using this modified microemulsion technique. © 2000 Elsevier Science B.V. All rights reserved.

Keywords: Nanocrystalline bismuth; Microemulsion; In situ polymerization; Semimetal; Quantum dot; Nanoparticle

1. Introduction

Crystalline materials exhibit a variety of interesting optical, electronic and magnetic effects when the physical size of the crystallite approaches the nanometer scale in at least one dimension; these phenomena are collectively known as quantum confinement effects. The most studied quantum-confined materials have been, of course, semiconductors and metals, but more recently the semimetal bismuth has received attention because of its highly anisotropic

electronic behavior, low conduction-band effective mass and high electron mobility [1]. In bulk Bi, the three conduction-band minima at the L point lie ≈ 40 meV lower than the single valence-band maximum at the T point [1,2]. Quantum confinement has been shown to convert Bi from a semimetal to a semiconductor in thin Bi layers grown by molecular beam epitaxy [3]. This size-induced semimetal to semiconductor transition and related quantum confinement effects are potentially useful for certain optical and electro-optical device applications [4]. In fact, thin films of Bi and $\text{Bi}_{1-x}\text{Sb}_x$ alloys have been shown to have among the largest third-order optical nonlinear susceptibilities at infrared wavelengths [5]. In addition to films, bismuth nanowires with 13 nm in diameter and 30–50 μm in length have been successfully prepared by injecting liquid Bi into nanometer scale channels of a porous anodic alumina

^{*} Corresponding author. Tel.: +1-504-280-6840; fax: +1-504-280-3185.

E-mail addresses: jfang1@uno.edu (J. Fang),
klstokes@uno.edu (K.L. Stokes)

template [6] or by electrodeposition of Bi into a porous alumina template [7]. The magnetoresistance of these materials has been studied [7–9] and it has been suggested that such a nanoscale bismuth system is attractive as a potential thermoelectric material [10].

Because of the intense interest in quantum-confined semimetal systems, we explore a low temperature, chemical approach for synthesizing nanometer-sized bismuth crystallites. Previously, colloidal bismuth particles (~ 20 nm in size) were produced by the radiolytic reduction of aqueous solutions [11]. However, these particles were investigated in solution and no attempt was made to extract the particles and study their structural properties. One difficulty is that the nanosized bismuth powder is quite unstable in air. Without protection against air, nanometer-sized bismuth particles are easily oxidized not only during the nucleation and growth process but also during the post-growth treatment stages. Therefore, it is worth designing a “coating layer” for protecting the nanoparticles.

In this letter, we demonstrate a technique to synthesize and isolate nanometer-sized bismuth particles. The particles are formed from the reduction of Bi salts in inverse micelles (water-in-oil inverse microemulsion). To limit oxidation of the fine Bi particles and prevent agglomeration, monomer precursors of poly(methyl methacrylate) (PMMA) are added to the oil phase of the microemulsion and polymerized in situ resulting in a polymeric network which surrounds and protects the Bi nanoparticles. The morphology and crystal structure of the crystallites is investigated with transmission electron microscopy (TEM) and X-ray diffraction (XRD). The results are compared to bismuth nanoparticles formed from a similar microemulsion route with no polymer encapsulation. We find that the polymer is effective in

protecting the particles against oxidation, especially during post-synthesis annealing.

2. Experimental procedure

The starting materials used in the present investigation include bismuth (III) nitrate ($> 98\%$ in purity), sodium borohydride (99.0% in purity), cyclohexane ($> 99.9\%$ in purity), methyl methacrylate (hereafter MMA) (99.0% in purity), 2-hydroxyethyl methacrylate (hereafter HEMA) ($> 99.0\%$ in purity), ethylene glycol dimethacrylate (98.0% in purity), 2,2-dimethoxy-2-phenylacetophenone (99.0% in purity, all above chemicals were from Aldrich, USA), ammonia solution (concentration: 28.0–30.0 wt.%, GR solution from EM Science), nitrate acid (concentration: 68.0–70.0 wt.%, GR solution from EM Science), and mixed poly(oxyethylene)₅ nonyl phenol ether (hereafter NP5) and poly(oxyethylene)₉ nonyl phenol ether (hereafter NP9) (in weight ratio: 2:1, Albright and Wilson Asia, Singapore).

To prevent from the formation of BiO^+ (bismuthyl ion) which is insoluble in water, the bismuth nitrate solution is made slightly acidic by adding nitric acid. The $[0.20 \text{ M Bi}(\text{NO}_3)_3 + 1.50 \text{ M HNO}_3]$ solution was prepared by dissolving 4.856 g $\text{Bi}(\text{NO}_3)_3 \cdot 5\text{H}_2\text{O}$ into 25.0 ml 3.0 M HNO_3 and such solution was diluted up to 50.0 ml using distilled water. The as-prepared solution was subsequently degassed using argon before the reaction. In order to increase the solubility of sodium borohydride in water and to neutralize the excess acid during the reaction, fresh $[1.00 \text{ M NaBH}_4 + 2.00 \text{ M NH}_3 \cdot \text{H}_2\text{O}]$ was prepared as well using argon-degassed distilled water.

Nanocrystalline bismuth was synthesized via two microemulsion processing routes. A simple mi-

Table 1
Weight ratio of each component in both microemulsion processing routes

System	Aqueous solution (12.0 wt.%)	Oil phase (66.0 wt.%)	Surfactant (22.0 wt.%)
ME-A	0.20 M $\text{Bi}(\text{NO}_3)_3$ + 1.50 M HNO_3	pure cyclohexane	14.7% NP5 + 7.3% NP9
ME-B	1.00 M NaBH_4 + 2.00 M $\text{NH}_3 \cdot \text{H}_2\text{O}$		
PME-A	0.20 M $\text{Bi}(\text{NO}_3)_3$ + 1.50 M HNO_3	49.8% cyclohexane + 12.4% MMA + 3.1% HEMA + 0.6% x-linker + 0.07% UV initiator	
PME-B	1.0 M NaBH_4 + 2.00 M $\text{NH}_3 \cdot \text{H}_2\text{O}$		

croemulsion route (hereafter ME) was used in which pure cyclohexane was employed as oil phase. An in situ polymerization–microemulsion synthesis (hereafter PME) was also used which contained a mixture of cyclohexane and monomers (in weight ratio of 3.2:1) as the oil phase. For each synthesis method, ME and PME, two microemulsion systems are prepared separately, one containing the dissolved

Bi^{3+} and the other containing the NaBH_4 reducing agent. The weight ratio of each component in each route is given in Table 1.

The procedure for establishing a partial phase diagram at room temperature for the ternary system consisting of oil phase (either pure cyclohexane or mixture of monomer components and cyclohexane), NP5 + NP9 and an aqueous solution has been de-

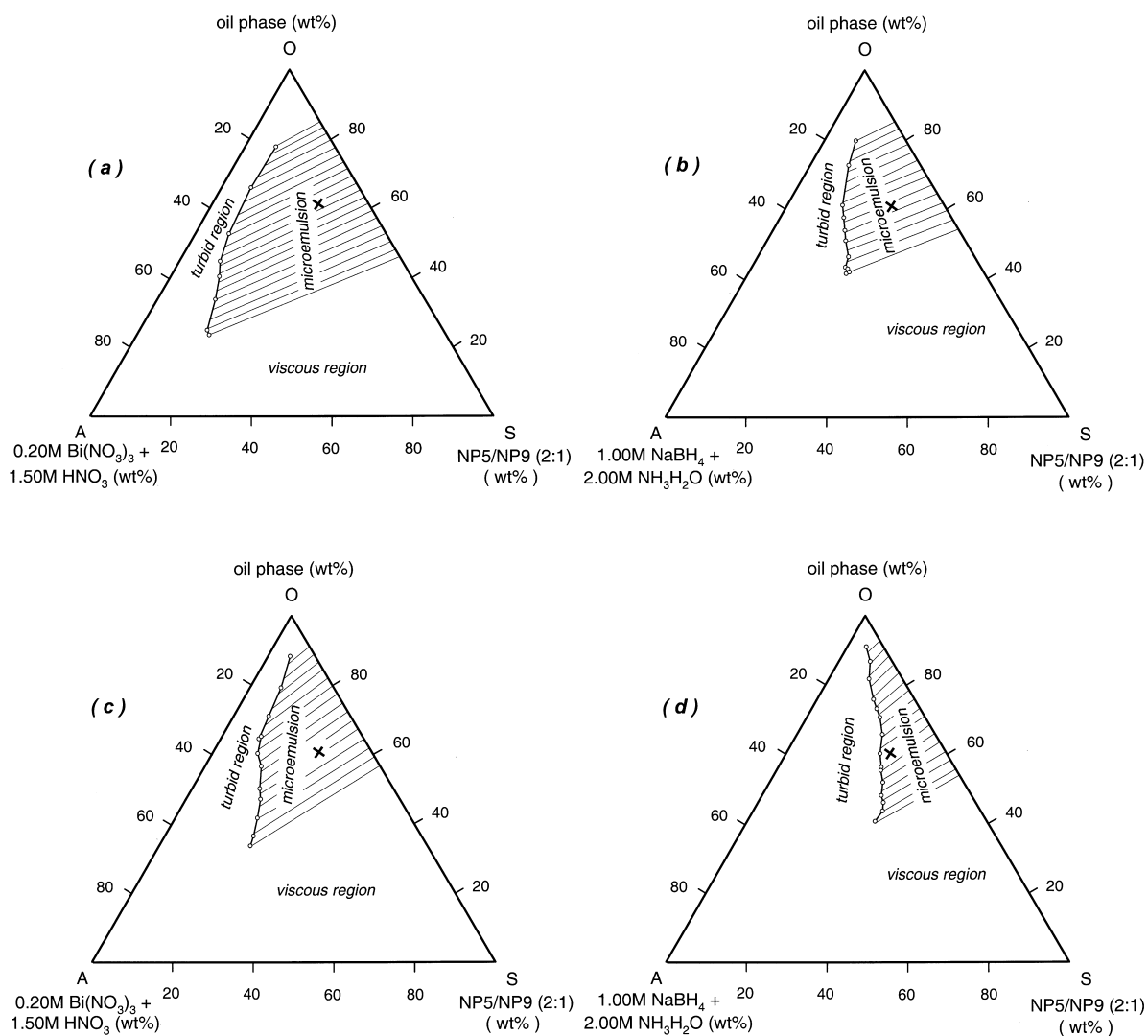


Fig. 1. Partial phase diagrams established at room temperature for the ternary systems consisting of (NP5 + NP9) surfactants, as well as various oil phase and aqueous solution. (a) oil phase: cyclohexane; aqueous solution: 0.20 M $\text{Bi}(\text{NO}_3)_3$ + 1.50 M HNO_3 . (b) oil phase: cyclohexane; aqueous solution: 1.00 M NaBH_4 + 2.00 M $\text{NH}_3\text{H}_2\text{O}$. (c) oil phase: 76 wt.% cyclohexane + 24 wt.% (4 MMA + HEMA); aqueous solution: 0.20 M $\text{Bi}(\text{NO}_3)_3$ + 1.50 M HNO_3 . (d) oil phase: 76 wt.% cyclohexane + 24 wt.% (4 MMA + HEMA); aqueous solution: 1.00 M NaBH_4 + 2.00 M $\text{NH}_3\text{H}_2\text{O}$.

tailed elsewhere [12,13]. To locate the demarcation between the microemulsion (transparent) and non-microemulsion (turbid) regions, the clear region was determined visually by titration of the aqueous solution into a mixture of oil and surfactant in given ratios in a screw-capped tube. Thorough mixing of the three phases was achieved using a Vortex mixer. Microemulsion compositions appear optically transparent when the size of aqueous droplets is in the 5 to 15 nm range, due to the fact that the nanosized aqueous droplets do not cause a substantial degree of light scattering. A series of such demarcation points (transition from transparent to turbid) were obtained by varying the weight ratio of oil phase to surfactant. The resulting phase diagrams are given in Fig. 1. In the following synthetic work, all the chosen microemulsion composition points are marked by "x" in Fig. 1(a,b,c,d) and are tabulated in Table 1.

In the ME route, two types of inverse microemulsions (designated ME-A and ME-B) were prepared. ME-A and ME-B contained two common components: the mixed non-ionic surfactants of NP5 and NP9 (in the weight ratio 2:1) and cyclohexane. The ME-A microemulsion consisted of an aqueous solution of 0.20 M $\text{Bi}(\text{NO}_3)_3$ and 1.50 M HNO_3 , whereas the ME-B microemulsion consisted of freshly prepared 1.00 M NaBH_4 in 2.00 M $\text{NH}_3 \cdot \text{H}_2\text{O}$ solution. The two microemulsions, ME-A and ME-B, were gradually mixed under argon gas while stirring. Two reactions occurred simultaneously: H^+ was neutralized by ammonia hydroxide, and Bi^{3+} was reduced into Bi by sodium borohydride resulting in very fine bismuth metal in black color. The pH value of final mixture was adjusted to $\text{pH} \approx 8$. After this colloidal system was destabilized by adding high purity ethanol, product was purified by centrifugation, followed by repeatedly washing using ethanol, distilled water and acetone successively, and a fine powder was obtained by vacuum-drying the sample for 24 h.

In the PME route, two inverse microemulsions were prepared as in the ME route. Microemulsion PME-A contained an aqueous phase of the bismuth ions and PME-B contained an aqueous phase of the borohydride. However, here the cyclohexane was partially replaced by polymerization agent in each microemulsion system as indicated in Table 1. MMA and HEMA were chosen as monomer and co-mono-

mer, respectively, ethylene glycol dimethacrylate as the cross-linker, and 2,2-dimethoxy-2-phenylacetophenone as UV initiator. When equal amounts of two microemulsions were similarly mixed under argon gas, the system was also irradiated with UV light for 20 min. In this case, nanoparticles of bismuth would form rapidly from the reduction, whilst polymerization takes place much more slowly. Polymer-coated nanosized bismuth could therefore be retrieved by performing post-purification as outlined above.

The as-dried specimens were annealed in argon at various temperatures, up to 240°C, for 2 h, followed by phase analysis and crystallite size estimation using XRD ($\text{CuK}\alpha$, Philips X'pert Systems) at room temperature. For TEM characterizations all specimens were sparingly dissolved in organic solvent (chloroform or a mixture of toluene and chloroform in 1:1) under ultrasonification. A drop of the resulting solution was dried onto a carbon coated TEM grid. A Jeol 2010 transmission electron microscope was employed to observe the particle morphology and to analyze the crystallinity.

3. Results and discussion

Fig. 1(a,b) shows the partial phase diagrams established at room temperature for the ternary system consisting of cyclohexane, NP5/NP9 and aqueous solution containing [0.20 M $\text{Bi}(\text{NO}_3)_3$ + 1.50 M HNO_3] and [1.00 M NaBH_4 + 2.00 M $\text{NH}_3 \cdot \text{H}_2\text{O}$], respectively. The microemulsion region, which is marked as shaded area in the diagrams, widens significantly with increasing NP5 + NP9 to cyclohexane ratio. For a given NP5 + NP9 to cyclohexane ratio, the microemulsion region in Fig. 2(a) is much wider than that in Fig. 2(b). This behavior can be explained by considering the interaction between the anions of the acidic aqueous phase and the hydrophilic end of the surfactant molecules compared to the interaction of the cations in the alkali aqueous phase with the surfactant molecules. In the microemulsion containing [0.20 M $\text{Bi}(\text{NO}_3)_3$ + 1.50 M HNO_3] (Fig. 1(a)), the ethylene oxide (EO) units $(-\text{O}-\text{CH}_2-\text{CH}_2-)_n$ of the mixed surfactants were "charged" by protonium ions (H_3O^+ from HNO_3). Such repulsion among the charged surfactant

molecules in the polar ends increases the water droplet size resulting in a widened microemulsion region. In the system containing [1.00 M NaBH_4 + 2.00 M $\text{NH}_3 \cdot \text{H}_2\text{O}$] (Fig. 1(b)), the cations can form strong complexes with EO units of the mixed surfactants [14]. In addition, the hydroxides (OH^-) may serve as weak bridge by linking the complexed cations of the neighboring surfactant molecules. The rigidity of the interfacial films of the inverse microemulsion droplets is thus increased, favoring the formation of smaller droplets of microemulsions. Therefore, the microemulsion region becomes narrow. Moreover, a previous study of similar microemulsion systems indicates that the microemulsion region would broaden as the concentration of alkali is decreased [15]. This assures that our mixed system in which the pH value was maintained around 8 remains a microemulsion as long as the system

points in two initial systems are controlled within microemulsion region. The investigation of phase behavior also reveals that the partial replacement of cyclohexane by the monomers results in a significant narrowing of microemulsion region in both the acidic system (Fig. 1(c)) and alkali system (Fig. 1(d)).

To study structural development of the bismuth nanoparticles prepared by both the ME and PME synthetic methods, the specimens were heated for 2 h under argon and followed by XRD phase analysis at room temperature. Fig. 2(a,b) are the XRD traces of both specimens at varying annealing temperatures. Without annealing treatment, broad XRD peaks can be observed in ME-derived sample as shown in Fig. 2(a) and these peaks are attributed to the formation of rhombohedral bismuth according to the standard ICDD PDF (Card No. 05-0519) even though a considerable amount of amorphous phase was simulta-

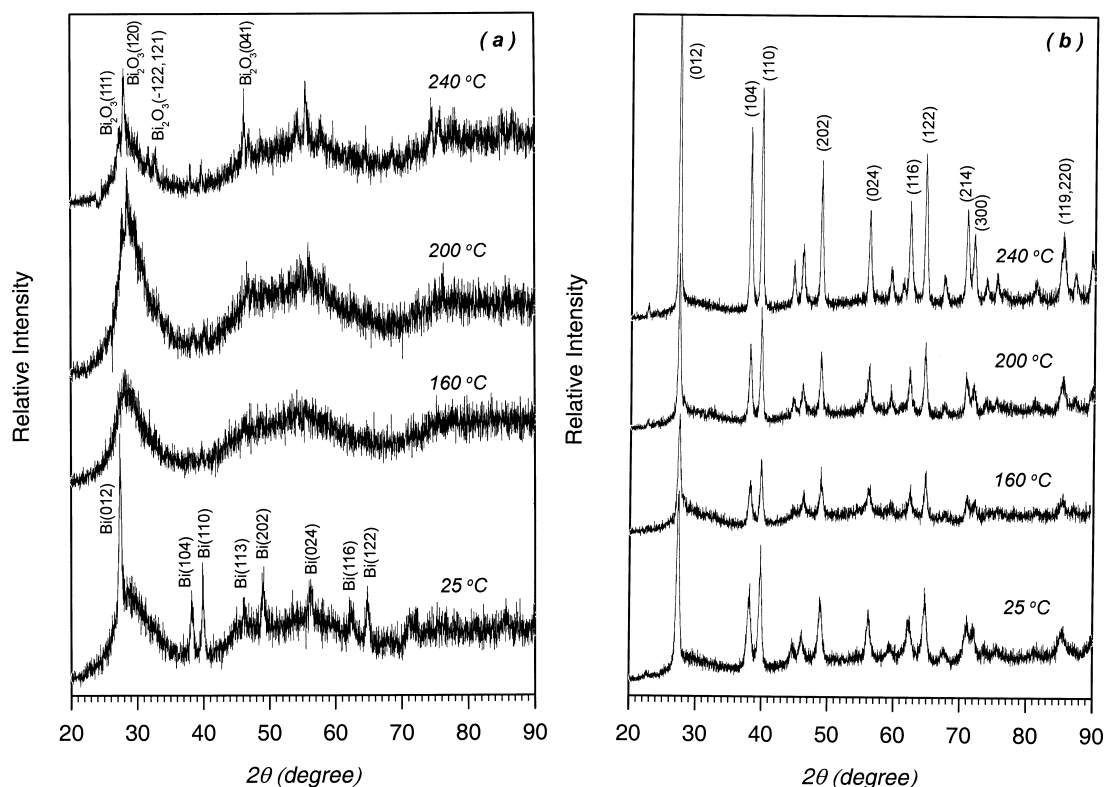


Fig. 2. (a, b) XRD traces of the as-prepared bismuth specimen via (a) ME and (b) PME process and those annealed at various temperatures for 2 h under argon atmosphere. (b) All the peaks are in agreement with diffraction peaks from rhombohedral bismuth; the main peaks are labeled.

neously indicated from this pattern. Applying the Scherrer equation [16] to the line broadening of the (012), (202) and (024) peaks, the average size of bismuth crystallites of this sample was estimated to be ~ 17 nm when the shape factor was regarded as 0.9. Fig. 2(a) also illustrates that the intensity of bismuth decreases with increased annealing temperature of the ME-derived specimens, and the peaks from rhombohedral bismuth phase completely vanish after annealing at 160°C . Further increase of the annealing temperature to 240°C results in a formation of bismuth oxide, which is represented by the typical peaks at $2\theta = 33.0^\circ$ ($-122,121$) and 46.3° (041) according to the standard ICDD PDF Card No. 41-1449. These variations in Fig. 2(a) reveal that nanophase of bismuth derived from ME route possesses a poor crystallinity and it is rather unstable during heating even in an argon atmosphere.

In contrast with ME-derived samples, PME-derived bismuth particles demonstrate a much higher crystallinity with a crystallite size as small as ~ 13 nm, as shown in Fig. 2(b). Increase of annealing temperature results in an enhancement of crystallinity accompanied by a slight increase in crystallite size as expected (see Table 2). A highly crystallized rhombohedral bismuth phase can be detected from the patterns of samples heated at 200°C or above. Moreover, no trace of bismuth oxide was detected in these XRD patterns. Comparison of these XRD patterns between ME- and PME-derived samples in Fig. 2 also indicates that in situ cross-linked polymer in this process becomes a network material which is able to protect the surface of bismuth particle from oxidation.

Fig. 3(a,b) show the transmission electron micrograph of ME-derived and PME-derived bismuth powders, respectively. As shown in Fig. 3(a), parti-

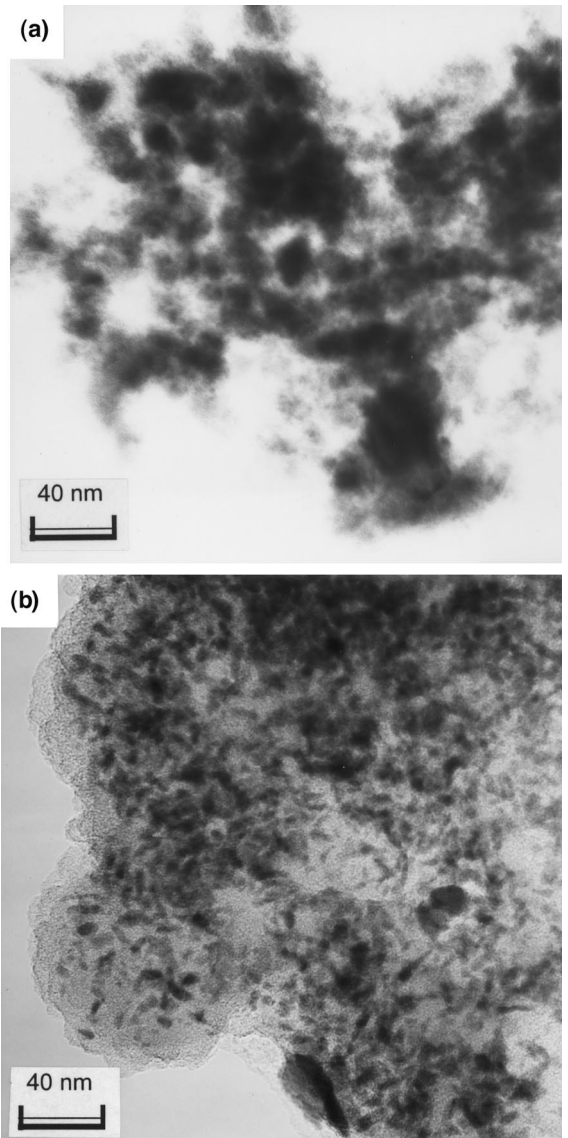


Fig. 3. TEM images of bismuth particles synthesized from (a) ME process; (b) PME process.

Table 2

Crystallite size of bismuth particles estimated from broadening of the XRD peaks

Annealing temperature	Average particle size (nm)	
	ME process	PME process
As prepared	16.8	13.2
160°C	–	15.3
200°C	–	22.6
240°C	–	23.9

cle agglomerates occur even though the primary particles of ME-derived bismuth are considerably very small. The ambiguousness of this morphology also indicates the presence of materials in amorphous phase. This observation is in good agreement with the XRD pattern in which amorphous phase was detected as dominant component. In contrast with ME-derived sample, discrete elongated particles

(rod-shaped) can be observed in the TEM of the PME-derived sample as shown in Fig. 3(b). The particles range about $\sim 5 \text{ nm} \times 20 \text{ nm}$ in size and are embedded in the polymeric network.

These observations indicate that in the synthesis of nanosized bismuth, introduction of an in situ polymerization process into the microemulsion reaction can efficiently restrict the growth of metal particles during the reaction, post purification and annealing processes. As mentioned above, XRD investigation suggests that highly crystalline bismuth particles are developed from the PME-derived sample. TEM dark diffraction also supports this result. It is not difficult to understand the difference in crystallinity between two samples prepared via PME and ME processes (with and without polymer stabilization). As suggested by previous researchers, inverse microemulsions consist of water droplets ranging from 5 to 15 nm [17,18]. Primary particles can be firstly formed within these water droplets, followed growth stages due to the dynamic nature and collision process among the water domains [19–21]. Eventually, each water domain in inverse microemulsions may contain few particles in the later reaction stage. Oxidation of the out-layer of bismuth particles, of course, will diminish the crystallinity and purity of bismuth. While in the case of PME process, since the formation of bismuth and the polymerization take place in different media, i.e., aqueous phase and oil phase, respectively, nanosized bismuth particles must be inlaid in the polymeric chains due to nature of microemulsion microstructure. If the polymer is cross-linked in inverse microemulsions, a well-dispersed porosity on the nanometer scale can be created for containing the bismuth particles. Such porous cross-linked polymer can actually be regarded as a networked material with Bi sites, which is shown in the TEM micrograph of Fig. 3(b). Nanosized particles of bismuth are thus isolated and protected by the polymeric network, and this structure can therefore avoid oxidation and particle growth during the annealing stage.

4. Conclusions

Nanometer-sized bismuth crystallites have been successfully synthesized using a modified inverse

microemulsion method with in situ polymerization. The greatly different reaction rates between the metal reduction ($\text{Bi}^{3+} \rightarrow \text{Bi}$) in the aqueous phase and polymerization in the organic phase allows bismuth nanoparticles to be grown surrounded by cross-linked PMMA network. Compared to bismuth nanoparticles synthesized from microemulsion without polymer, the polymer-coated nanoparticles are protected from oxidation and show high crystallinity and purity of single phase. This synthesis technique provides a viable route for the formation of highly crystalline bismuth nanoparticles which can serve as the basis for further studies of quantum-confined bismuth.

Acknowledgements

This work was supported by research grant DAAD19-99-1-0001 from the Army Research Office. We would also like to thank Dr. Thomas Kodenkandath, Dr. John Wiley and Dr. Matthew A. Tarr for their kind support in providing a furnace and UV source.

References

- [1] C.F. Gallo, B.S. Chandrasekhar, P.H. Sutter, *J. Appl. Phys.* 34 (1963) 144.
- [2] J.-P. Issi, *Aust. J. Phys.* 32 (1979) 585.
- [3] C.A. Hoffman, J.R. Meyer, F.J. Bartoli, A. Di Venere, X.J. Yi, C.L. Hou, H.C. Wang, J.B. Ketterson, *Phys. Rev. B* 48 (1993) 11431. *Phys. Rev. B* 51 (1995) 5535.
- [4] T.D. Golding, J.A. Dura, H. Wang, J.T. Zborowski, A. Vigilante, H.C. Chen, J.H. Miller Jr., J.R. Meyer, *Semicond. Sci. Technol.* 8 (1993) S117.
- [5] E.R. Youngdale, J.R. Meyer, C.A. Hoffman, F.J. Bartoli, D.L. Partin, C.M. Thrush, J.P. Heremans, *Appl. Phys. Lett.* 59 (1991) 756.
- [6] Z. Zhang, J.Y. Ying, M.S. Dresselhaus, *J. Mater. Res.* 13 (1998) 1745.
- [7] K. Hong, F.Y. Yang, K. Liu, D.H. Reich, P.C. Searson, C.L. Chien, F.F. Balakirev, G.S. Boebinger, *J. Appl. Phys.* 58 (1999) 6184.
- [8] K. Liu, C.L. Chien, P.C. Searson, *Phys. Rev. B* 58 (1998) 14681.
- [9] Z. Zhang, X. Sun, M.S. Dresselhaus, J.Y. Ying, J.P. Heremans, *Appl. Phys. Lett.* 73 (1998) 1589.
- [10] M.S. Dresselhaus, Z. Zhang, X. Sun, J. Ying, J.P. Heremans, G. Dresselhaus, G. Chen, in: *Thermoelectric Materials 1998*, T.M. Tritt (Ed.), *Mater. Res. Soc. Symp. Proc.* 5451999, p. 215.

- [11] M. Gutiérrez, A. Henglein et al., *J. Phys. Chem.* 100 (1996) 7656.
- [12] L.M. Gan, L.H. Zhang, H.S.O. Chan, C.H. Chew, B.H. Loo, *J. Mater. Sci.* 31 (1996) 1071.
- [13] J. Fang, J. Wang, S.-C. Ng, C.-P. Chew, L.-M. Gan, *Nanostruct. Mater.* 8 (1997) 499.
- [14] G.K. Lim, J. Wang, S.C. Ng, C.H. Chew, L.M. Gan, *Biomaterials* 18 (1997) 1433.
- [15] J. Fang, *Processing of Functional Ceramics via Microemulsion Routes*, Chap. 3, *Microemulsion Systems for Producing Ultrafine Ceramic Materials*, PhD Thesis, National Univ. of Singapore, 1998.
- [16] H.P. Klug, L.E. Alexander, in: *X-Ray Diffraction Procedures for Polycrystalline and Amorphous Materials*, Wiley, New York, 1954, pp. 491–538.
- [17] L. Auvray, in: W.M. Gelbart, A. Beu-Shaul, D. Roux (Eds.), *Micelles, Membranes, Emulsions and Monolayers*, Springer, New York, 1994.
- [18] L.M. Gan, C.H. Chew, in: H.S. Nalwa (Ed.), *Advanced Functional Molecules and Polymers*, Gordon and Breach Science Publishers, 1999, in press.
- [19] P.D.I. Flecher, B.H. Robinson, F. Bermejo-Barrera, D.G. Oakenfull, in: I.D. Robb (Ed.), *Microemulsions*, Plenum, New York, 1982, p. 221.
- [20] H.G. Thomas, A. Lomakin, D. Blankschtein, G.B. Benedek, *Langmuir* 13 (1997) 209.
- [21] C. Tojo, M.C. Blanco, F. Rivadulla, M.A. López-Quintela, *Langmuir* 13 (1997) 1970.